UNSTEADY LAMINAR CONVECTION FLOW OVER PERIODIC GROOVES BY USING SIO_2-WATER NANOFLUID

AMIRHOSSEIN HESHMATI[1], MOHAMMAD PARSAZADEH[2] & FARSHID FATHINIA[3]

[1,2&3]Department of Mechanical Engineering, University Technology Malaysia, Johor, Malaysia
E-mail:pmohammad4@live.utm.my

Abstract—unsteady laminar forced convection flow in a 2-dimensional channel over periodic grooves is numerically investigated. Finite volume method is used and the equations were discretized by second order upwind method. The rib-height to channel-height ratio (B/H) is 2. The downstream wall is heated by a uniform heat flux while the upstream wall is insulated. Quasi steady point was obtained at τ=10. The heat transfer is analyzed with different nanoparticles volume fraction and diameter of 0-4% and 20nm-50nm for SiO_2 respectively at Reynolds number of 400 and τ=10. Water is used as a base fluid of nanoparticles. The results revealed 124% heat transfer enhancement compared to the water in a grooved channel by using SiO_2 nanoparticle with volume fraction and nanoparticle diameter of 4% and 20nm respectively.

Keywords—*Unsteady, Forced convection, Periodic grooves, Nanofluids, Heat transfer*

I. INTRODUCTION

The improvement of heat transfer has been paid more attention due to increasing the engineering applications. One of the common passive ways to enhance the heat transfer is using the roughen surfaces, grooves, baffles, and ribs to produce local turbulent flow or disturb~~ing~~ the flow.

High performance of various engineering applications is owed to the efficient heat transfer enhancement. Grooved channels have a significant role in this sort of heat transfer enhancement. Energy system equipment, electronic cooling, cooling of nuclear reactors, cooling of turbine blades, combustion chambers, environmental control systems are the beneficial samples of this method [1].

Analyzing the thermal and flow field over groove channel has been experimentally and numerically done by investigators since last two decades. Eiamsa and Promvonge [2] have investigated flow and thermal behavior of forced convection of an incompressible airflow in a 2-dimensional channel with 9 periodic transverse grooves on its lower wall. They found that reverse re-circulation flow can considerably increase heat transfer in a transverse grooves channel.

Adachi et al. [3] presented the effect of expanded grooves on pressure drop determined in a horizontal channel including 54 grooves sets to measure the pressure drop even for small Reynolds numbers. Adachi and Uehara [4] studied Correlation between heat transfer and pressure drop in 2-dimensional horizontal channels using fully developed flow with periodically grooved parts.

A considerable effect on heat transfer was seen by changing rib shapes. Rib-Triangular groove (RR-TG), Triangular rib-Triangular groove (TR-TG) and Triangular rib-Rectangular groove (TR-RG) were three shapes that having mounted on the lower wall of channel and analyzed with a turbulent flow by Eiamsa and Promvonge [5]. They found that Rectangular rib-Triangular groove (RR-TG) has highest heat transfer. They also studied the effects of pitch ratio on heat transfer rate for these three geometries. In a similar effort Kamali and Binesh [6] studied effects of square, trapezoidal and triangular rib shapes with decreasing height, while increasing height was in trapezoidal rib shape numerically, on characteristics of turbulent incompressible airflow in a 2-dimensional horizontal ribbed channel, while uniform heat flux was imposed on lower wall and upper wall was maintained in an adiabatic condition. They concluded the highest mean Nusselt number and enhancement factor were for trapezoidal rib with decreasing height. Effects of Reynolds number and wall thermal conductivity ratio to the fluid and geometric parameters on heat transfer for rectangular and arc-shaped grooves have been reported by Shokouhmand et al. [7]. Heat transfer in an intermittently and symmetrically grooved channel with 7 contiguous triangular grooves followed by a flat section in the range of Reynolds number varying between 600 and 1,800 was investigated by Greiner et al. [8]. Their results revealed that Nusselt number is went up with increasing Reynolds number.

As for flow characteristics effects, modifying the topology of grooved channel is another way to increase the heat transfer, having been utilized by researchers during last decades. Herman and Kang [9] experimentally studied forced convection cooling of electrical components in grooved channels with three different topologies of basic grooved channel (BGC), grooved channel with cylindrical eddy promoters (GCC) and grooved channel with curved vanes (GCV) in laminar, transitional and turbulent airflows in the range of 200 to 6,500 Reynolds

number. They reported BGC is the best for moderate to high Reynolds numbers while GCV has the optimum performance. They also investigated the heat transfer performance of grooved channel by attaching curved vanes at downstream of each block. The goal of using curved vanes in this experiment was to enhance heat transfer at flank regions and eliminate large recirculation zone in grooves. Ortiz et al. [10] have investigated the heat transfer enhancement in a 2-dimensional horizontal grooved channel by attaching curved deflectors. They revealed that in basic grooved channels; flow after passing over a rib directly hits the next rib, is heated, gets trapped and creates recirculation flow.

Some researchers have focused on utilizing nanofluids to increase heat transfer parameters. Oronzio et al. [11] studied the effect of nanofluids on ribbed channel numerically and found that heat transfer is improved. Al-aswadi et al. [12] investigated numerically forced convection flow over backward facing step by using nanofluids. In their research water was base fluid and Au, Ag, Cu, CuO, Al_2O_3, SiO_2, TiO_2, and diamond were nanoparticles. They concluded SiO_2 have generally improved the heat transfer.

It is clear from above studies that conventional fluids have been used to investigate the characteristics of heat transfer and using nanofluids flow was not analyzed on grooved channel in unsteady laminar condition and it has motivated the current study. Al-aswadi et al. [12] reported that SiO_2 provides highest heat transfer enhancement compared to some other nanoparticles. So, in the present study, 2-dimentional numerical simulations over periodic grooves in a horizontal channel are carried out with SiO_2 as nanoparticle that volume fraction and nanoparticle diameter varied 1-4% and 20-50nm respectively. Water was used as the base fluid under study. The purpose of this study is to obtain the Nusselt number and skin friction coefficient of the considered Nanofluid with different nanoparticle diameter and nanoparticle concentration along the channel for laminar unsteady flow.

II. MODEL DESCRIPTION AND GOVERNING EQUATIONS

The schematic of interested system is shown in Fig. 1. This channel was fixed by nine grooves and 8 ribs along the downstream channel wall. The channel length, rib land (s) is set to be 1870 mm and 5H/4 respectively. The channel height is H=40mm, while groove width (B) is fixed to 3H/4. The entry length of 20H is considered to create a fully developed flow. The last groove is located to 10H upstream of the exit. The length of test section and rib height was 670 mm and H/2 mm, respectively. This geometry has been fixed by eight ribs with the length of 50mm (s=5H/4). The groove width ratio, (B/H), is located to be B/H=0.75. Foregoing geometrical dimensions and heat flux are the same as grooved channel of smith and Pongjet [2].

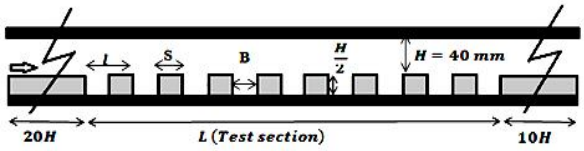

Fig. 1 Grooved channel

TABLE I
NOMENCLATURE

Symbol	Quantity
B	distance between grooves
t	time
D_h	hydraulic diameter of channel
e	rib height or groove depth
cf	skin friction coefficient
H	channel height
h	convective heat transfer coefficient
k	thermal conductivity
L	channel length of test section
Nu	Nusselt number
p	static pressure
Re	Reynolds number
s	rib land/length
T	temperature
U	mean velocity
u'_i	fluctuation velocity components
μ	kinematic viscosity
R	eddy viscosity
τ_{ij}	specific gas constant
□	wall shear stress
Cp	thermal enhancement factor
Cv	specific heat at constant volume
ρ	specific heat at constant volume
γ	density
l	ratio of heat capacities
q	groove and rib land
	heat flux

The governing equations under consideration of the steady 2-dimensional incompressible form of Continuity equation, Navier-Stokes equations and Energy equation are as [13]:

Continuity equation:

$$\frac{\partial \rho}{\partial t} + \frac{\partial}{\partial x_i}(\rho u_i) = 0 \quad (1)$$

Momentum equation:

$$\frac{\partial(\rho u_i)}{\partial t} + \frac{\partial(\rho u_i u_j)}{\partial x_i} = -\frac{\partial p}{\partial x_i} + \frac{\partial \tau_{ij}}{\partial x_i} + \rho g \delta_{i2} \quad (2)$$

Energy equation:

$$\frac{\partial T}{\partial x_i} + \frac{\partial(u_i T)}{\partial x_i} = (1 - \frac{R}{C_v}) T \frac{\partial u_i}{\partial x_i} - \frac{\gamma}{\rho c_p} \frac{\partial q_i}{\partial x_i} \quad (3)$$

where u_i is the velocity vector in the x_i direction, P is the pressure, ρ is the density, R is the specific gas constant, γ is the ratio of heat capacities, c_v and c_p

are the specific heat at constant volume and specific heat at constant pressure respectively.

Viscous stress tensor and heat flux are presented respectively as:

$$\tau_{ij} = \mu\left[\frac{\partial u_i}{\partial x_j} + \frac{\partial u_j}{\partial x_i} - \frac{2}{3}\delta_{ij}\frac{\partial u_k}{\partial x_k}\right] \quad (4)$$

and

$$q_i = -k\frac{\partial T}{\partial x_i} \quad (5)$$

where μ and k are dynamic viscosity and thermal conductivity respectively.

The density of nanofluid can be obtained from [14]:

$$\rho_{nf} = (1-\phi)\rho_f + \phi\rho_{np} \quad (6)$$

where ρ_f and ρ_{np} are mass densities of base fluid and NPs, respectively.

The effective heat capacity is given as [14]:

$$(\rho C_p)_{nf} = (1-\phi)(\rho C_p)_f + \phi(\rho C_p)_{np} \quad (7)$$

Where $(\rho C_p)_f$ and $(\rho C_p)_{np}$ are heat capacities of base fluid and Nanoparticles, respectively.

The effective thermal conductivity equation of nanofluid is writen as [14]:

$$k_{eff} = k_{static} + k_{Brwnian} \quad (8)$$

$$k_{static} = k_f\left[\frac{(k_{np}+2k_f) - 2\phi(k_f - k_{np})}{(k_{np}+2k_f) + \phi(k_f - k_{np})}\right] \quad (8.1)$$

$$k_{Brwnian} = 5\times10^4\beta\phi\rho_f C_{p,f}\sqrt{\frac{KT}{2\rho_{np}R_{np}}}f(T,\phi) \quad (8.2)$$

where K_{np} and K_f are the thermal conductivities of nanoparticles and base fluid respectively.

Boltzman Constant:

$$k = 1.3807\times10^{-23}\ J/K \quad (8.3)$$

$$f(T,\phi) = (2.8217\times10^{-2}\phi + 3.917\times10^{-2})\left(\frac{T}{T_0}\right) + (-3.0669\times10^{-2}\phi - 3.391123\times10^{-2}) \quad (8.4)$$

for $1\% \le \phi \le 4\%$ and 300K , where T is the fluid temperature, and T_0 is the reference temperature.

The effective viscosity can be obtained using following mean empirical correlations [14]:

$$\mu_{eff} = \mu_f \times \frac{1}{(1-34.87(d_p/d_f)^{-0.3}\times\varphi^{1.03})} \quad (9)$$

$$d_f = \left[\frac{6M}{N\pi\rho f_0}\right]^{\frac{1}{3}} \quad (9.1)$$

where M is the molecular weight of base fluid, N is the Avogadro number, and ρ_{f0} is the mass density of the based fluid calculated at temperature T_0=293K.

The effective thermal expansion is expressed as [14]:

$$(\rho\beta)_{nf} = (1-\phi)(\rho\beta)_f + \phi(\rho\beta)_{np} \quad (10)$$

for different particle materials the β equations are listed in Table II.

TABLE II

β VALUES FOR DIFFERENT PARTICLES

Type of particles	β	*Concentration (%)*
SiO_2	$1.9526(100\phi)^{-1.4594}$	$1\% \le \varphi \le 10\%$

III. NUMERICAL IMPLEMENTATION

Governing equations is solved by finite volume method using SIMPLE algorithm. The normalized residual values are converged at 10^{-3} for all variables. Second order upwind method numerical approaches have been implemented for convective and diffusive terms, respectively. Besides, researchers have implicitly applied the discretized nonlinear equations. The pressure–velocity coupling algorithm SIMPLE (Semi Implicit Method for Pressure-Linked Equations) was chosen to evaluate the pressure field. At the inlet, uniform velocity profile has been imposed. Impermeable boundary condition over the channel wall is implemented while a constant heat flux condition is applied to over lower wall to create a thermally developed condition [2].

In this case three parameters have been presented, velocity profile, skin friction coefficient and Nusselt number. Skin friction coefficient is calculated by shear stress over the test section as [2]:

$$c_f = \frac{\tau_w}{1/2\,\rho u^2} \quad (15)$$

where τ_w is shear stress, ρ and u are density and velocity, respectively. The local Nusselt number is defined by:

$$Nu(x) = \frac{h(x)D_h}{k} \quad (16)$$

and average Nusselt number can be calculated by:

$$Nu = \frac{1}{l}\int Nu(x)dx \quad (17)$$

IV. GRID TESTING AND CODE VALIDATION

Grid testing is implemented using several mesh sizing and densities to guarantee a grid independent solution. Air is used as a gird testing fluid with four different grids sizes of 30,225 cells, 51,050 cells, 94,050 cells, and 104,800 cells are selected to

compare their local Nusselt numbers with the RNG k−ε turbulence model. Fig. 2 represents various local Nusset numbers of different grid sizes. The results revealed that after 94,050 cells, the difference between results is less than 4%. Therefore, mentioned grid size is chosen which separate the results dependence from grid size.

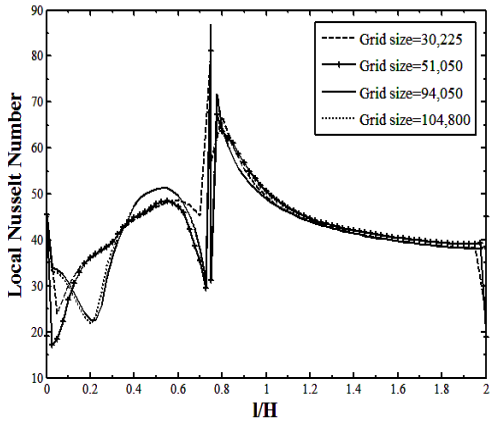

Fig. 2 Effect of grid size on local Nusselt number at Re=9000

Fig. 3 shows the accuracy of the selected grid size. The deviation of this study and referred study is slightly increased with the raise of Reynolds number. However, this percentage of deviation is less than 5% which can be evidenced that the results of the foregoing grid size are in accordance with Smith and Pongjet study [2].

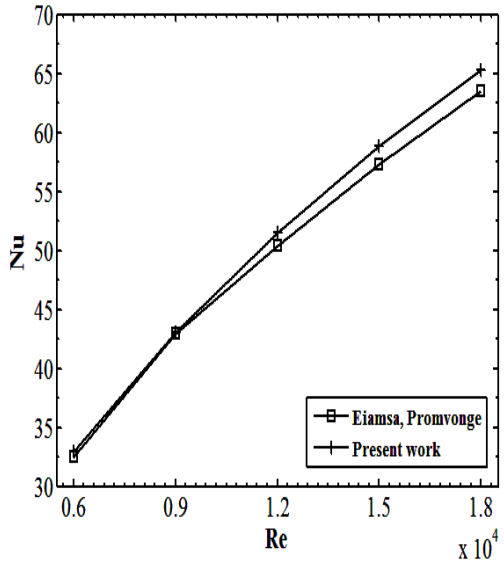

Fig. 3 Validation of local Nusselt numbers at different Reynolds number

V.RESULTS AND DISCUSSION

The unsteady flow simulation is done for SiO_2 nanoparticle and nanoparticle concentration of 1% to 4% and nanoparticle diameter varied from 20nm to 50nm . Water used as a base fluid for Nanofluid mixture in a Reynolds number of 400.

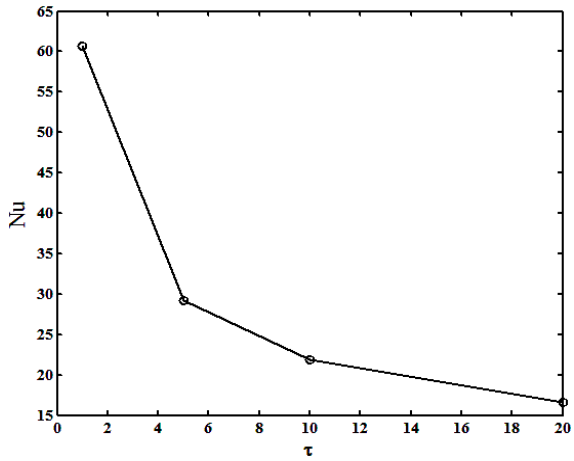

Fig. 4 Average Nusselt number of SiO_2, Ø=4% and dp=20nm

Average Nusselt numbers and skin friction coefficients of laminar forced convection and unsteady flow for SiO_2 with 4% nanoparticle concentration and 20nm nanoparticle diameter in four different time (τ=1,5,10,20) and Reynolds number of 400 in a grooved channel is illuminated in Fig. 4-6. Steady state flow is the time that all derivatives of time are totally disappeared and no change observed with changing the time at a specific point. According to such a definition, the result indicates that the average Nusselt number and skin friction coefficient are independent and slightly varied since τ=10. Furthermore, the velocity profile at middle of the rib 4 and groove 5 are shown in Fig. 6(rib 4 and groove 5 is chosen to effects of rib and groove channel totally reflected to the working fluid). A huge variation is seen when the τ varied from 1 to 5 which this alteration was seen for average Nusselt number and skin friction coefficient that this change decreased as τ change from 5 to 10 which proves the unsteady condition for working fluid. Eventually, independence of the velocity profile from time variation is seen for both rib and groove since τ=10. So, this time can be called quasi steady state that the fluid properties almost do not change over time. According to such a notion, quasi steady state point can be implemented to further investigation.

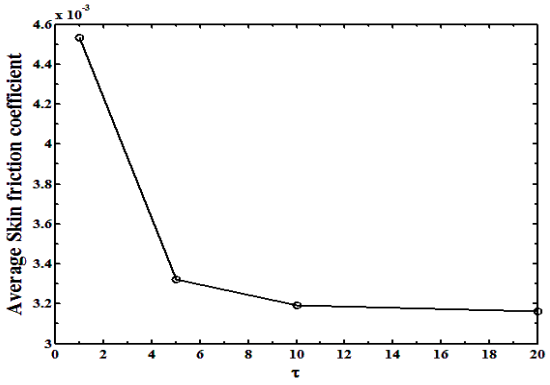

Fig. 5 Average skin friction coefficient of SiO_2-water with Ø=4% and dp=20nm

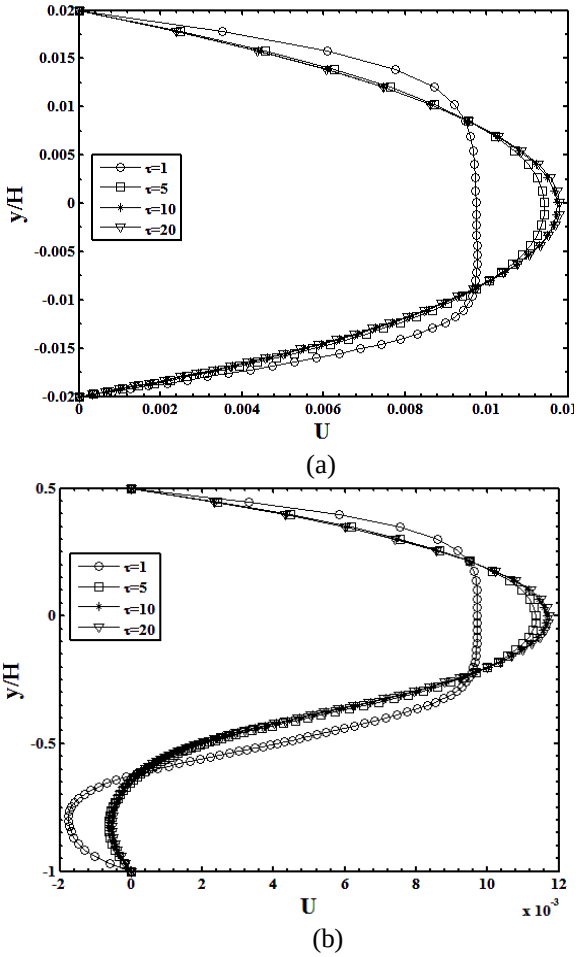

Fig. 6 Different times of velocity profile of groove 5 for SiO_2-water with Ø=4% and dp=20nm (a) rib 4 (b) groove 5

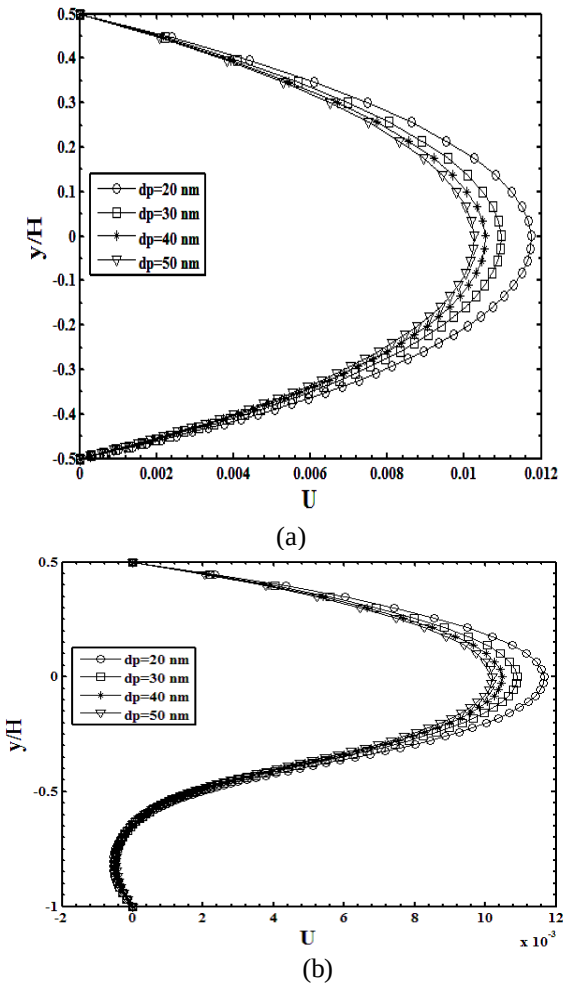

Fig. 7 Effect of Different nanoparticle diameters on velocity profile for SiO_2-water with Ø=4% (a) rib 4 (b) groove 5

Fig.7 depicts different nanoparticle diameters varied from 20nm to 50nm for SiO_2-water Nanofluid and its effects on velocity profile of rib 4 and groove 5 at Reynolds number of 400. It would be eminent that velocity profile shapes for all nanoparticle diameters are similar. It means that there is no recirculation or vortex is produced by changing nanoparticle diameter However, velocity increases with decreasing nanoparticle diameter. Moreover, a fluctuation on groove velocity profile is observed due to the reversed flow having produced on groove channel which strongly affect on velocity profile. The results reveal that nanoparticle diameter of 20nm provides more velocity than other nanoparticle diameters in both rib and groove sections.

Average Nusselt number of SiO_2-water Nanofluid for nanoparticle diameter varied from 20nm to 50nm at nanoparticle concentration of 4% and Reynolds number of 400 in a grooved channel is shown in Fig. 8.a. Obviously, Nusselt number decrease with increasing nanoparticle diameter. A significant reason of such a Nusselt number reduction is due to the velocity reduction having mentioned before. A part from that, thermal conductivity of the Nanofluid mixture plays a significant role on heat transfer enhancement. In this case, higher thermal conductivity is provided by stronger Browninan motion at smaller nanoparticle diameters [15].

Fig. 8.b illuminates average skin friction coefficient of the SiO_2-water nanofluid at the same condition as Nusselt number. The figure shows effectiveness of the skin friction coefficient with nanoparticle diameters that average skin friction coefficient increase with decreasing nanoparticle diameter due to the increasing shear stress over the test section by increasing nanoparticle diameter.

Fig. 9 indicates the effects of nanoparticle concentrations on velocity profile for SiO_2-water nanofluid varied from 0% (pure water) to 4% at nanoparticle diameter of 20nm in a grooved channel. According to the no changes on the velocity profile appearance is seen by changing the volume fraction; so, no difference exists on streamlines of the working fluid flow. However, the velocity increases with increasing nanoparticle concentration. Highest velocity is achieved at

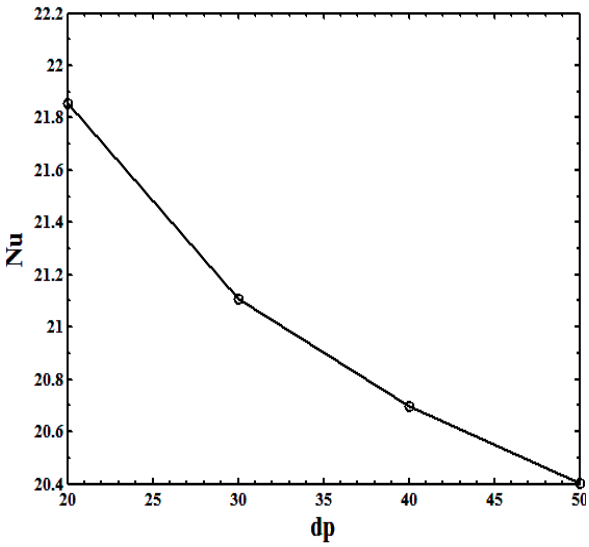

(a)

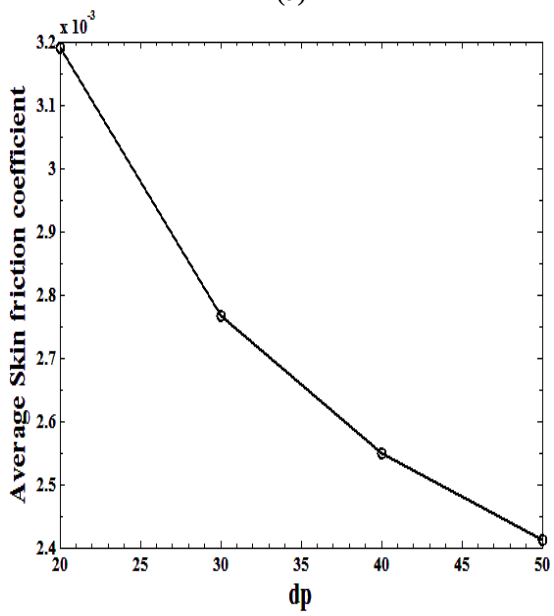

(b)

Fig. 8 (a) Average Nusselt number (b) Average skin friction coefficient of SiO_2,for different nanoparticle diameters with ∅=4%

volume fraction of 4% for both rib and groove velocity profiles.

Variety volume fraction affect on average Nusselt number and skin friction coefficient at fixed Reynolds number having shown in Fig. 4.10. It would be obvious that increasing volume fraction caused to heat transfer enhancement and higher average skin friction coefficient. A main reason of such an augmentation on heat transfer is that higher volume fraction provides higher velocity which strongly affect on heat transfer enhancement. Furthermore, higher volume fraction has higher dynamic and static thermal conductivities which in turn increase average Nusselt number.

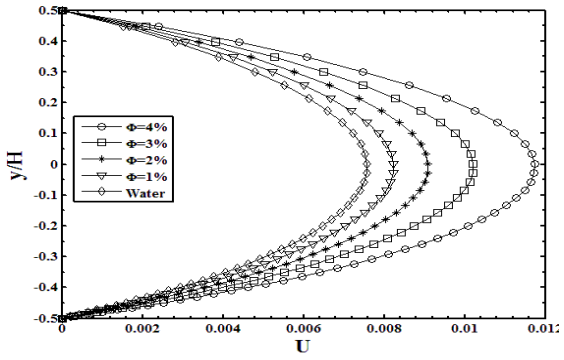

(a)

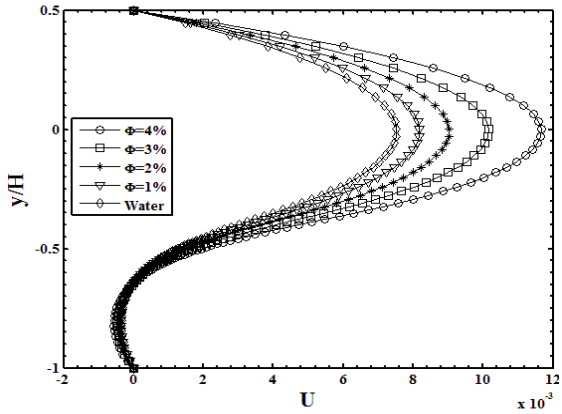

(b)

Fig. 9 Effects volume fractions on velocity profile for SiO_2-water with ∅=4% (a) rib 4 (b) groove 5

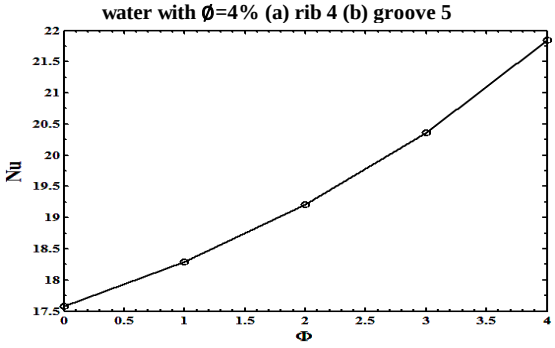

(a)

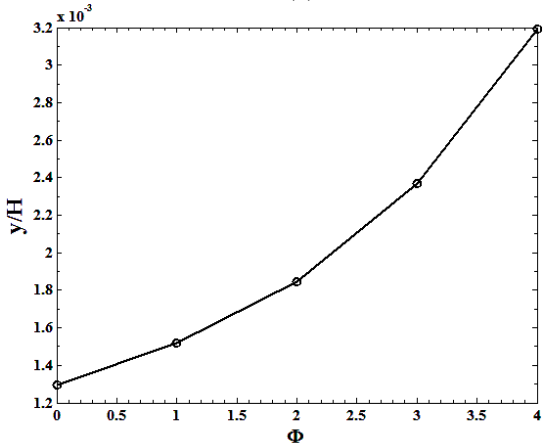

(b)

Fig. 10 (a) Average Nusselt number (b) Average skin friction coefficient of SiO_2, for different nanoparticle volume fraction at dp=4%

VI. CONCLUSION

In the present investigation, a numerical simulation of 2-dimensional unsteady laminar forced convection flow over periodic grooves in a horizontal channel heated by a uniform heat flux on grooved wall and insulated upper wall was conducted at B/H=0.75. Second order upwind method was chosen to equations discretization. Quasi steady point was obtained at τ=10. Varieties SiO2 nanoparticles characteristics with water as base fluid were chosen and compared with pure water to identify the appropriate nanoparticle characteristics at τ=10. Since skin friction friction coefficient was reported for all nanoparticles characteristics of SiO_2. Eventually, the 4% volume fraction and 20nm nanoparticle diameter provided highest heat transfer enhancement and skin friction coefficient in unsteady laminar forced convection flow.

REFERENCES

[1] Ankit Kumar, A.K.D., Effect of a circular cylinder on separated forced convection at a backward-facing step. International Journal of Thermal Sciences,Vol. 52, p. 9, 2012.

[2] S.Eiamsa-ard ,P.Promvonge, Numerical study on heat transfer of turbulent channel flow over periodic grooves. International Communications in Heat and Mass Transfer, 35, pp. 844-852, 2008.

[3] T.Adachia, Y.Tashiroa, H.Arimab, Y.Ikegami(2009), Pressure drop characteristics of flow in a symmetric channel with periodically expanded grooves, Chemical Engineering Science, vol.64, pp. 593—597, 2009.

[4] T.Adachi, H.Uehara , Correlation between heat transfer and pressure drop in channels with periodically grooved parts, International Journal of Heat and Mass Transfer, vol. 44, 2001.

[5] S.Eiamsa-ard, P.Promvonge, Thermal characteristics of turbulent rib-grooved channel flows, International Communications in Heat and Mass Transfer, vol. 36, pp. 705–711, 2009.

[6] J R. Kamali ,A.R. Binesh, The importance of rib shape effects on the local heat transfer and flow friction characteristics of square ducts with ribbed internal surfaces, International Communications in Heat and Mass Transfer, vol. 35, pp. 1032–1040, 2008.

[7] H.Shokouhmand ,K.Vahidkhah, M.A.Esmaeili, Numerical Analysis of Air Flow and Conjugated Heat Transfer in Internally Grooved Parallel- Plate Channels, World Academy of Science, Engineering and Technology, vol. 73, 2011.

[8] M.Greiner, F,Fischer,M.Tufo, Two-Dimensional Simulations of Enhanced Heat Transfer in an Intermittently Grooved Channel, Journal of Heat Transfer, Vol. 124, June 2002.

[9] M C. Herman, E. Kang , Comparative evaluation of three heat transfer enhancement strategies in a grooved channel, Heat and Mass Transfer, vol. 37 , pp.563-575, 2001.

[10] L.Ortiz, A. Hernandez-Guerrero, C. Rubio-Arana, R. Romero-Mendez, Heat transfer enhancement in a horizontal channel by the addition of curved deflectors, International Journal of Heat and Mass Transfer, vol. 51, pp. 3972–3984, 2008.

[11] Oronzio Manca, S.N., Daniele Ricci, A numerical study of nanofluid forced convection in ribbed channels. Applied Thermal Engineering,vol. 37, pp. 280-292, 2012.

[12] A.A. Al-aswadi, H.A.M., N.H. Shuaib, Antonio Campo, Laminar forced convection flow over a backward facing step using nanofluids. International Communications in Heat and Mass Transfer, vol 37, 2010.

[13] Héctor Barrios-Pina, Stéphane Viazzo, Claude Rey, A numerical study of laminar and transitional mixed convection flow over a backward-facing step, J Computers & Fluids, vol 56,pp. 77–91, 2012.

[14] S A.Sh. Kherbeet , H.A.M., B.H. Salman, The effect of nanofluids flow on mixed convection heat transfer over microscale backward-facing step. International Journal of Heat and Mass Transfer, 2012.

[15] H.R Seyf, M.Feizbakhshi,'' Computational Analysis of Nanofluid Effects on Convective Heat Transfer Enhancement of Micro-Pin-Fin Heat sinks'', International Journal of Thermal Sciences, vol,58,2012,pp168-179.